


# Possible effect of static surface disorder on diffractive scattering of H<sub>2</sub> from Ru(0001): Comparison between theory and experiment

Cite as: J. Chem. Phys. **147**, 244705 (2017); <https://doi.org/10.1063/1.5011741>

Submitted: 02 November 2017 . Accepted: 11 December 2017 . Published Online: 29 December 2017

G. J. Kroes , Mark Wijzenbroek, and J. R. Manson 

## COLLECTIONS

 This paper was selected as Featured



View Online



Export Citation



CrossMark

## ARTICLES YOU MAY BE INTERESTED IN

[Methane dissociation on the steps and terraces of Pt\(211\) resolved by quantum state and impact site](#)

The Journal of Chemical Physics **148**, 014701 (2018); <https://doi.org/10.1063/1.5008567>

[Ab initio molecular dynamics study of the Eley-Rideal reaction of H + Cl-Au\(111\) → HCl + Au\(111\): Impact of energy dissipation to surface phonons and electron-hole pairs](#)

The Journal of Chemical Physics **148**, 014702 (2018); <https://doi.org/10.1063/1.5016054>

[Communication: Counter-ion solvation and anomalous low-angle scattering in salt-free polyelectrolyte solutions](#)

The Journal of Chemical Physics **147**, 241103 (2017); <https://doi.org/10.1063/1.5010784>

The Journal  
of Chemical Physics

2018 EDITORS' CHOICE

READ NOW!



# Possible effect of static surface disorder on diffractive scattering of H<sub>2</sub> from Ru(0001): Comparison between theory and experiment

G. J. Kroes,<sup>1</sup> Mark Wijzenbroek,<sup>1</sup> and J. R. Manson<sup>2,3</sup>

<sup>1</sup>*Leiden Institute of Chemistry, Gorlaeus Laboratories, Leiden University, P.O. Box 9502, 2300 RA Leiden, The Netherlands*

<sup>2</sup>*Department of Physics and Astronomy, Clemson University, Clemson, South Carolina 29634, USA*

<sup>3</sup>*Donostia International Physics Center (DIPC), Paseo Manuel de Lardizabal, 4, 20018 Donostia-San Sebastian, Spain*

(Received 2 November 2017; accepted 11 December 2017; published online 29 December 2017)

Specific features of diffractive scattering of H<sub>2</sub> from metal surfaces can serve as fingerprints of the reactivity of the metal towards H<sub>2</sub>, and in principle theory-experiment comparisons for molecular diffraction can help with the validation of semi-empirical functionals fitted to experiments of sticking of H<sub>2</sub> on metals. However, a recent comparison of calculated and Debye-Waller (DW) extrapolated experimental diffraction probabilities, in which the theory was done on the basis of a potential energy surface (PES) accurately describing sticking to Ru(0001), showed substantial discrepancies, with theoretical and experimental probabilities differing by factors of 2 and 3. We demonstrate that assuming a particular amount of random static disorder to be present in the positions of the surface atoms, which can be characterized through a single parameter, removes most of the discrepancies between experiment and theory. Further improvement might be achievable by improving the accuracy of the DW extrapolation, the model of the H<sub>2</sub> rotational state distribution in the experimental beams, and by fine-tuning the PES. However, the question of whether the DW model is applicable to attenuation of diffractive scattering in the presence of a sizable van der Waals well (depth  $\approx$  50 meV) should also receive attention, in addition to the question of whether the amount of static surface disorder effectively assumed in the modeling by us could have been present in the experiments. *Published by AIP Publishing.* <https://doi.org/10.1063/1.5011741>

## I. INTRODUCTION

The diffractive scattering of H<sub>2</sub> from metal surfaces has been studied experimentally for a large number of systems,<sup>1-4</sup> including H<sub>2</sub> + Ru(0001),<sup>5,6</sup> Pt(111),<sup>7</sup> Pd(111),<sup>8</sup> Cu(111),<sup>9</sup> and Ru/Cu(111).<sup>9</sup> Part of the motivation for this work comes from findings that specific features of the diffraction, such as the strength of the out-of-plane diffraction intensities, can serve as fingerprints of the reactivity of the metal surface studied towards dissociative chemisorption.<sup>4,9</sup> Additionally, in principle, the comparison of computed diffraction probabilities to measured values should enable a rigorous assessment of the potential energy surface (PES) used in the dynamics calculations employed to calculate the theoretical data. The reason for this is that computed diffraction probabilities are quite sensitive to the details of the PES and much more sensitive than computed reaction probabilities.<sup>4,6,10</sup> Specifically, changing the density functional on which the PES is based from PW91<sup>11</sup> to RPBE<sup>12</sup> may lead to qualitative differences in the dependence of computed diffraction probabilities on incidence energy, while at best quantitative differences (mostly an energy shift of the reaction probability curve) are observed for reaction, as has been demonstrated for H<sub>2</sub> + Ru(0001)<sup>6</sup> and Cu(111).<sup>10</sup> In principle, this makes the calculation of diffraction probabilities and their subsequent comparison to accurate experimental data a useful tool to validate electronic structure approaches to calculating

molecule-metal surface interaction potentials, such as the specific reaction parameter approach to density functional theory (SRP-DFT).<sup>13,14</sup>

In the SRP-DFT approach, typically a parameter in a density functional is fitted by requiring that computed sticking probabilities reproduce measured molecular beam sticking probabilities to within chemical accuracy (1 kcal/mol).<sup>13,14</sup> Next, the SRP density functional is validated by showing that with the functional thus obtained, an experiment to which the functional was not fitted can be reproduced to within similar accuracy.<sup>13,14</sup> Research on reactive and diffractive scattering of H<sub>2</sub> from Pt(111),<sup>7</sup> which established that with a specific PES both molecular beam sticking probabilities and diffraction probabilities could be reproduced semi-quantitatively, suggested that diffraction experiments can also be used to validate candidate SRP-density functionals. However, whereas recent dynamics calculations<sup>15</sup> were able to derive candidate SRP density functionals with which molecular beam sticking probabilities<sup>16</sup> could be reproduced to high accuracy for both H<sub>2</sub> and D<sub>2</sub> + Ru(0001), they failed to achieve good agreement with measured diffraction probabilities for H<sub>2</sub> + Ru(0001)<sup>6</sup> (see also Fig. 1). In particular, the computed elastic scattering probabilities overestimated the measured specular scattering probabilities by about a factor two and the measured first order diffraction probabilities by about a factor 3. A recently derived SRP density functional for H<sub>2</sub> + Pt(111) likewise allowed molecular beam sticking probabilities<sup>17</sup> to be

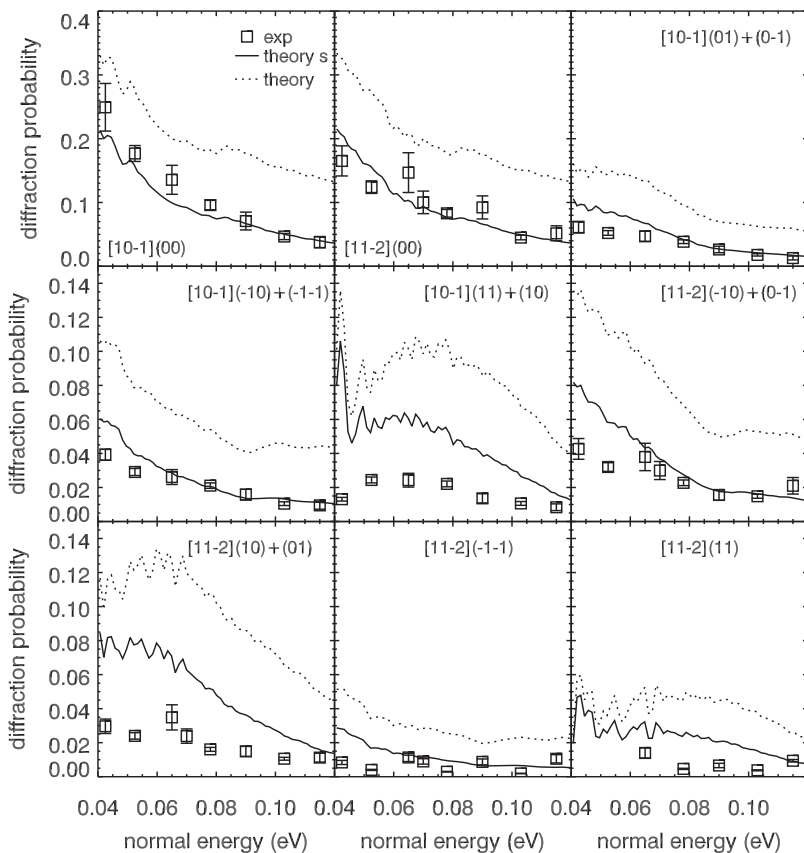


FIG. 1. Diffraction probabilities computed for  $n$ -H<sub>2</sub> scattering from Ru(0001) with an initial parallel translational energy of 35 meV in the  $[10\bar{1}]$  and  $[11\bar{2}]$  incidence directions, as computed with the PBE:RPBE(50:50)-vdW-DF XC functional and for the transitions indicated. The dotted lines represent the original results obtained in Ref. 15. The solid lines represent the computed results scaled with a Debye-Waller-type attenuation factor describing the effect of static surface disorder. Experimental results<sup>6</sup> are shown as square points with error bars.

reproduced for both normal and off-normal incidence,<sup>18</sup> but when combined with the Born-Oppenheimer Static Surface (BOSS) model failed to accurately describe measured Debye-Waller (DW) extrapolated<sup>7</sup> diffraction probabilities for this system.<sup>18</sup>

In the analysis of the discrepancies between theory and experiment for diffractive scattering of H<sub>2</sub> from Ru(0001), several potential causes for the discrepancies have been discussed.<sup>15</sup> In the light of the sensitivity of computed diffraction results to the PES employed, as alluded to earlier, one obvious potential cause is that the obtained candidate SRP density functionals are simply not accurate enough yet to allow a precise quantitative description of diffractive scattering. Another possible, but rather unlikely, cause is that  $n$ -H<sub>2</sub> used in the experiments was modeled as consisting of 25%  $J = 0$  and 75%  $J = 1$  H<sub>2</sub>, thereby neglecting contributions from  $J = 2$  and  $J = 3$  H<sub>2</sub>. Finally, while measured reaction probabilities (or reaction probabilities inferred from associative desorption probabilities assuming detailed balance) typically show no<sup>17</sup> or only little<sup>19,20</sup> dependence on surface temperature ( $T_s$ ), measured diffraction probabilities exhibit a strong exponential dependence on  $T_s$  known as Debye-Waller attenuation.<sup>3</sup> To enable the comparison between the theory for a static Ru(0001) surface and experiment, the measured diffraction probabilities had to be extrapolated from the value of  $T_s$  at which they were measured (500 K) down to 0 K. (The value of 500 K for  $T_s$  was needed to keep the surface clean from hydrogen.<sup>5</sup>) As the Debye-Waller model employed accurately described the attenuation of measured diffraction probabilities going from  $T_s = 1000$  to 500 K,<sup>6</sup> it was not immediately clear why this

extrapolation might fail when extended to lower temperatures. However, an alternative cause for the noted discrepancies, i.e., a type of static surface disorder could lead to attenuation through diffusive scattering, was not yet considered in the analysis.<sup>15</sup>

Here, we consider the possibility that the discrepancies observed between the calculations based on the SRP density functional<sup>15</sup> and the experiments<sup>6</sup> on diffraction of H<sub>2</sub> scattering from Ru(0001) are due to diffusive scattering from a randomly disordered surface.<sup>21</sup> As we will show below, the type of static disorder we consider leads to an additional type of Debye-Waller-like attenuation of the diffraction probabilities. However, this additional attenuation is not dependent on  $T_s$ , rather a static roughness displacement factor  $a_\ell$  takes on the role of the  $T_s$ -dependent phonon displacement in the Debye-Waller-type attenuation factor. This displacement factor is treated as an adjustable parameter and fitted to obtain optimal agreement between the theoretical and experimental specular scattering probabilities for the two high symmetry incidence conditions considered in the experiments. Next, we investigate to what extent this also improves the agreement between theory and experiment for lowest order non-specular diffraction for these two incidence directions.

This paper is set up as follows. Section II A briefly describes the dynamical model previously used to compute diffraction probabilities, including the quantum dynamics method employed. Section II B is somewhat longer as it describes how we extend the theoretical treatment to take into account the effect of a possible random type of static surface disorder. Sections II C and II D describe the PES employed

and the computational details of the previous work; again, these are short as little has changed relative to the earlier work. Section III A describes how taking into account random static surface disorder through a single adjustable parameter affects the agreement between theory and experiment. As we will show, the agreement between theory and experiment is improved dramatically, although not all problems are solved yet. Section III B provides additional discussion by considering what types of effects could lead to a static surface disorder of the type and magnitude needed to bring about the observed agreement. This section also discusses what other types of effects might be responsible for at least the remaining discrepancy with experiment. Section IV presents our conclusions and a brief outlook.

## II. METHOD

### A. Model and quantum dynamics calculations

In the previous work calculating reaction and diffraction probabilities for  $\text{H}_2 + \text{Ru}(0001)$ , the Born-Oppenheimer static surface (BOSS) model was used.<sup>4,13</sup> This means that the possible effects of electron-hole pair excitation and of energy transfer involving surface phonons have been neglected in the calculation of observables. The quality of these approximations for reactive scattering of  $\text{H}_2$  from a metal surface has been discussed before, for instance, in Ref. 22, to which we refer the reader for a detailed discussion. In the BOSS model, the only degrees of freedom left are the six degrees of freedom of the molecule, and the coordinate system that was used in the dynamical calculations and in the calculation of the PES is shown in Fig. 2(a).

Whereas surface phonons can be neglected in calculations aimed at simulating molecular beam sticking probabilities of  $\text{H}_2$  on cold metal surfaces,<sup>4</sup> it has been known for a long time that measured diffraction probabilities need to be Debye-Waller (DW) extrapolated to 0 K to enable quantitative comparisons with theory (see, for instance, Ref. 23). As

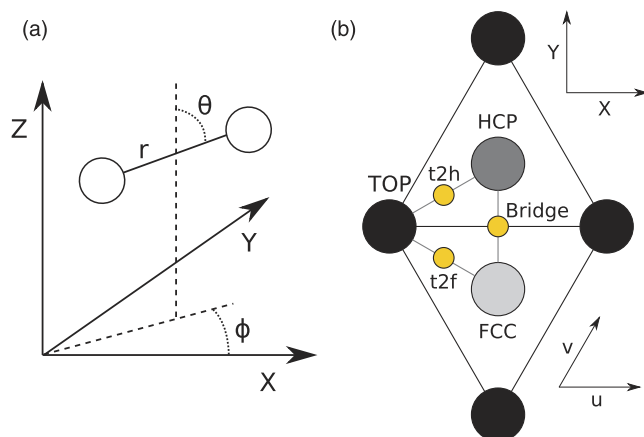


FIG. 2. (a) The six-dimensional coordinate system used in the dynamics calculations on and PES construction for  $\text{H}_2$  scattering from  $\text{Ru}(0001)$ .<sup>15</sup> (b) Top view of the  $\text{Ru}(0001)$  surface unit cell. In the (0001) surface of the hcp  $\text{Ru}$  crystal, the hcp site corresponds to a second-layer atom, and the fcc site corresponds to an empty site (stacking ABAB...).

discussed in Ref. 6, DW attenuation describes the  $T_s$  dependence of specular scattering probabilities rather well between 500 K (at which the measurements were done) and 1000 K. The experimental diffraction probabilities were therefore extrapolated down to 0 K using fitted values of the van der Waals potential well depth and the surface Debye temperature of  $60 \pm 5$  meV and  $473 \pm 2$  K, respectively.<sup>6</sup> Assuming that the experimental results are also influenced by the type of static surface disorder discussed in Sec. II B, the theoretically computed diffraction probabilities need to be multiplied with an additional attenuation factor, which will be discussed in Sec. II B.

To define incidence directions and diffractive transitions, the conventions were adopted that apply to fcc metal surfaces like  $\text{Pt}(111)$  (see also Fig. 2 of Ref. 6), of course realizing that  $\text{Ru}$  is an hcp metal. Specifically, the  $[10\bar{1}]$  incidence direction is defined by a plane that is normal to the surface along the top-bridge-top direction, where the top sites indicated are nearest neighbor surface atoms [see Figs. 2(b) and 3(a)]. The  $[11\bar{2}]$  incidence direction is defined by a plane that is normal to the surface along the top-hcp-bridge-fcc-top direction, where the top sites indicated are second nearest neighbor surface atoms [see also Figs. 2(b) and 3(a)]. The diffractive transitions are visualized with reference to these incidence directions in Fig. 3(b).

Diffraction probabilities were previously computed with the time-dependent wave packet (TDWP) method<sup>24</sup> as implemented for  $\text{H}_2$  scattering from a surface within the BOSS dynamical model, while treating all six molecular degrees of freedom without further approximations.<sup>25</sup> Specifically, diffraction probabilities  $P_{nm}(v, J, m, j)$  are computed for the

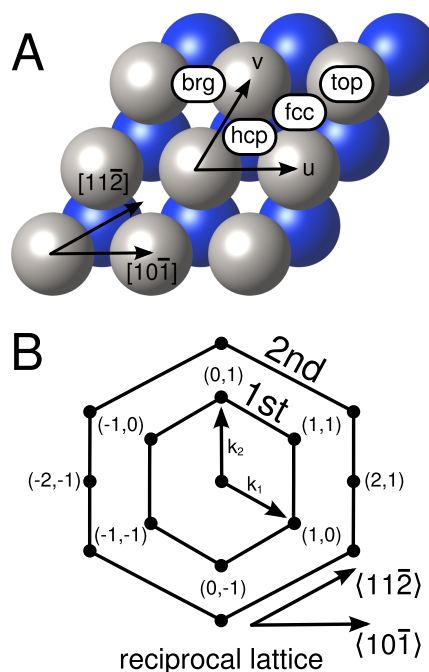


FIG. 3. Conventions used here and in previous work<sup>5,6,15</sup> to define the incidence directions and diffractive transitions for  $\text{H}_2 + \text{Ru}(0001)$  in real space (a) and in reciprocal space (b). In the real-space non-orthogonal coordinate system  $(u, v)$ , the  $u$  and  $v$  axes make an angle of  $60^\circ$  with one another, and  $u$  is along the  $X$  axis in Fig. 2.

vibrational state  $v = 0$  and for the combinations  $(J, m_J) = (0, 0)$ ,  $(1, -1)$ ,  $(1, 0)$ , and  $(1, 1)$  of the rotational and magnetic rotational quantum number. To mimic the rotationally elastic diffractive scattering of  $n\text{-H}_2$ , for each diffraction state  $(n, m)$ , these diffraction probabilities are averaged over the four  $(J, m_J)$  states indicated. More details of the dynamics calculations are presented in Sec. II D.

## B. Static surface disorder in diffractive scattering

As discussed above, the calculations of Refs. 6 and 15 for  $\text{H}_2$  scattering from Ru(0001) were carried out without considering thermal displacements due to phonon vibrations. With respect to vibrations, the target surface was frozen. However, as also already noted, at temperatures above ambient, the thermal attenuation behavior of the experimental data reported in Ref. 6 accurately obeyed that of a Debye-Waller factor whose temperature dependence is well known. Because the temperature dependence of all measured diffraction peaks was well defined by the Debye-Waller behavior, it was possible to extrapolate all experimental diffraction peak intensities to their expected value for a frozen surface, i.e., even the effects of zero point motion were eliminated. With this extrapolation, the experiment provides data that can be quantitatively compared with the frozen surface calculations. However, at best this procedure eliminates the effects of thermal disorder; it does not account for the possibility of residual static disorder that may be inherent in the surface. Here we show how static disorder may be included as an additional attenuating factor that multiplies each diffraction peak. The approach follows well-known treatments of scattering of waves from rough surfaces, where the attenuating factor is typically called a characteristic function.<sup>21</sup>

The starting point is the quantum mechanical transition rate for a molecular projectile to scatter from an initial state of translational momentum  $\hbar\mathbf{k}_i$  to the final state of  $\hbar\mathbf{k}_f$ ,

$$w(\mathbf{k}_f, \mathbf{k}_i) = \left\langle \frac{2\pi}{\hbar} |T_{fi}|^2 \delta(E_f - E_i) \right\rangle, \quad (1)$$

where  $T_{fi}$  is the transition matrix,  $E_{f,i}$  are the final and initial kinetic energies, and the brackets  $\langle \rangle$  indicate an average over the distribution of static disorder. The actual quantity to be compared with experimentally measured scattering intensities is the differential reflection coefficient, which is the transition rate multiplied by a Jacobian whose only  $\mathbf{k}$ -dependence is the ratio  $|\mathbf{k}_f|/k_{iz}$  where the perpendicular component of the incident wave vector  $k_{iz}$  is proportional to the incident flux. The interaction potential can be written as a two-dimensional summation over unit cells of the periodic surface, denoted by the two-dimensional number  $\ell$ ,

$$V(\mathbf{r}) = \sum_{\ell} V^{uc}(\mathbf{r} - \mathbf{R}_{\ell} - \mathbf{a}_{\ell}). \quad (2)$$

In Eq. (2), the notation *uc* stands for the surface unit cell. The two-dimensional displacement vector  $\mathbf{R}_{\ell}$  denotes the position of the  $\ell$ th unit cell on the surface and  $\mathbf{a}_{\ell}$  is the small three-dimensional static displacement vector of that cell due to disorder. With a potential of this form, it is reasonable to assume that the transition operator can be written in the same form,

$$\hat{T} = \sum_{\ell} \hat{T}^{uc}(\mathbf{r} - \mathbf{R}_{\ell} - \mathbf{a}_{\ell}), \quad (3)$$

essentially casting the interaction into a form similar to the kinetic approximation that has been successful in describing low energy electron diffraction (LEED).<sup>26</sup>

The transition matrix element is evaluated with respect to unperturbed plane wave states,

$$\begin{aligned} T_{fi} &= \langle \Phi_f | \hat{T}(\mathbf{r}) | \Phi_i \rangle = \int d\mathbf{r} e^{-i\mathbf{k}_f \cdot \mathbf{r}} \hat{T}(\mathbf{r}) e^{i\mathbf{k}_i \cdot \mathbf{r}} \\ &= \sum_{\ell} e^{-i\Delta\mathbf{k} \cdot (\mathbf{R}_{\ell} - \mathbf{a}_{\ell})} \int d\mathbf{r} e^{-i\Delta\mathbf{k} \cdot \mathbf{r}} \hat{T}^{uc}(\mathbf{r}) \\ &\equiv \sum_{\ell} e^{-i\Delta\mathbf{k} \cdot (\mathbf{R}_{\ell} - \mathbf{a}_{\ell})} T_{fi}^{uc}, \end{aligned} \quad (4)$$

where  $\Delta\mathbf{k} = \mathbf{k}_f - \mathbf{k}_i$  is the scattering vector. With Eq. (4) the transition rate of Eq. (1) becomes

$$\begin{aligned} w(\mathbf{k}_f, \mathbf{k}_i) &= \frac{2\pi}{\hbar} \sum_{\ell} \sum_m e^{-i\Delta\mathbf{k} \cdot (\mathbf{R}_{\ell} - \mathbf{R}_m)} \langle e^{-i\Delta\mathbf{k} \cdot \mathbf{a}_{\ell}} e^{i\Delta\mathbf{k} \cdot \mathbf{a}_m} \rangle \\ &\quad \times |T_{fi}^{uc}|^2 \delta(E_f - E_i). \end{aligned} \quad (5)$$

One cannot assume quantum mechanical commutation between displacements at different sites, but this is readily handled using the Baker-Hausdorff relation,

$$e^A e^B = e^{A+B} e^{[A,B]/2}, \quad (6)$$

which is valid if the commutator  $[A,B]$  is a *c*-number. Then the average over small displacements involves only averages over exponentials of  $\mathbf{a}_{\ell}$ . If  $\mathbf{a}_{\ell}$  are random displacements, i.e., Gaussian distributed, then the average is carried out using the well-known relation

$$\langle e^A \rangle = e^{\langle A^2 \rangle / 2}. \quad (7)$$

With the above two relations, the average over small displacements in the transition function of Eq. (5) is evaluated as

$$\langle e^{-i\Delta\mathbf{k} \cdot \mathbf{a}_{\ell}} e^{i\Delta\mathbf{k} \cdot \mathbf{a}_m} \rangle = e^{-\langle (\Delta\mathbf{k} \cdot \mathbf{a}_{\ell})^2 \rangle} e^{\langle \Delta\mathbf{k} \cdot \mathbf{a}_{\ell} \Delta\mathbf{k} \cdot \mathbf{a}_m \rangle}. \quad (8)$$

Since all unit cells are subject to a small random displacement with respect to each other governed by one and the same Gaussian distribution function, the self-correlation function of each unit cell  $\langle (\Delta\mathbf{k} \cdot \mathbf{a}_{\ell})^2 \rangle$  is independent of lattice site  $\ell$  so it can be written as  $\langle (\Delta\mathbf{k} \cdot \mathbf{a})^2 \rangle$ . Furthermore, if the displacements are small, the site-site correlation function will also be small and one can make the expansion

$$\langle e^{-i\Delta\mathbf{k} \cdot \mathbf{a}_{\ell}} e^{i\Delta\mathbf{k} \cdot \mathbf{a}_m} \rangle = e^{-\langle (\Delta\mathbf{k} \cdot \mathbf{a})^2 \rangle} \{1 + \langle \Delta\mathbf{k} \cdot \mathbf{a}_{\ell} \Delta\mathbf{k} \cdot \mathbf{a}_m \rangle + \dots\}. \quad (9)$$

As will become clear below, the lowest order term in this expansion contributes only to diffraction. The higher order terms in Eq. (9) contribute to elastic diffusive scattering in all directions. To understand this, note that a single displaced unit cell acts as a point defect that weakly breaks the symmetry of an ordered surface, and such a point defect scatters in all directions according to its cross section. The first order term  $e^{-\langle (\Delta\mathbf{k} \cdot \mathbf{a})^2 \rangle} \langle \Delta\mathbf{k} \cdot \mathbf{a}_{\ell} \Delta\mathbf{k} \cdot \mathbf{a}_m \rangle$  in Eq. (9), when substituted back into the transition rate of Eq. (5), leads to the first order Born approximation to the diffuse elastic scattering due to the random disorder.



Since the only contribution of interest here is the diffraction, the transition rate of Eq. (5) simplifies to

$$w^{(0)}(\mathbf{k}_f, \mathbf{k}_i) = \frac{2\pi}{\hbar} e^{-\langle(\Delta\mathbf{k}\cdot\mathbf{a})^2\rangle} \sum_{\ell} \sum_m e^{-i\Delta\mathbf{k}\cdot(\mathbf{R}_{\ell}-\mathbf{R}_m)} \times |T_{fi}^{uc}|^2 \delta(\varepsilon_f - \varepsilon_i). \quad (10)$$

The remaining sums over lattice sites parallel to the surface are straightforward to evaluate and lead to the conditions that the parallel component  $\mathbf{K}$  of the scattering vector can only be a reciprocal lattice vector  $\mathbf{G}$  of the surface,

$$\sum_{\ell} \sum_m e^{-i\Delta\mathbf{k}\cdot(\mathbf{R}_{\ell}-\mathbf{R}_m)} = N \sum_n e^{-i\Delta\mathbf{k}\cdot\mathbf{R}_n} = N^2 \sum_{\mathbf{G}} \delta_{\mathbf{K},\mathbf{G}}, \quad (11)$$

where  $N$  is the number of surface unit cells, which can be viewed as the total area of the surface divided by the area of a single unit cell.

Thus, the final form for the transition rate for diffraction becomes

$$w(\mathbf{k}_f, \mathbf{k}_i) = \frac{2\pi N^2}{\hbar} \sum_{\mathbf{G}} e^{-\langle(\Delta\mathbf{k}\cdot\mathbf{a})^2\rangle} |T_{fi}^{uc}|^2 \delta_{\mathbf{K},\mathbf{G}} \delta(\varepsilon_f - \varepsilon_i). \quad (12)$$

The above equation has the same form as the well-known exact form for diffractive scattering from a surface. The two-dimensional periodic symmetry implies the conservation of parallel momentum modulo a surface reciprocal lattice vector and this, as well as the conservation of energy, is expressed by the two  $\delta$  functions. The intensity of each diffraction peak is governed by the form factor of a single unit cell, which is  $|T_{fi}^{uc}|^2$ . The remaining factor is the attenuation  $\exp\{-\langle(\Delta\mathbf{k}\cdot\mathbf{a})^2\rangle\}$  that accounts for the reduction in intensity of each diffraction peak due to diffusive scattering by the disorder, essentially that due to higher order terms ignored in Eq. (9). Since the scattered intensity is proportional to the transition rate, this implies that the intensity of a given diffraction peak  $I_{\mathbf{G}}$  is attenuated due to the disorder in the following manner:

$$I_{\mathbf{G}} = I_{\mathbf{G}}^0 e^{-\langle(\Delta\mathbf{k}\cdot\mathbf{a})^2\rangle}, \quad (13)$$

where  $I_{\mathbf{G}}^0$  is the corresponding diffraction intensity for a perfectly ordered surface. Explicitly written out in Cartesian coordinates,

$$\Delta\mathbf{k}\cdot\mathbf{a} = (k_{fz} - k_{iz})a_z + G_x a_x + G_y a_y, \quad (14)$$

with the final normal momentum given according to the energy and momentum conservation conditions,

$$k_{fz}^2 = k_{iz}^2 + \mathbf{K}_i^2 - (\mathbf{K}_i + \mathbf{G})^2, \quad (15)$$

and it is noted that surface scattering is a back-scattering configuration for which  $k_{iz}$  and  $k_{fz}$  are in opposite directions so that

$$\Delta k_z = k_{fz} - k_{iz} = |k_{fz}| + |k_{iz}|. \quad (16)$$

In evaluating  $\langle(\Delta\mathbf{k}\cdot\mathbf{a})^2\rangle$ , terms arrive such as  $\langle a_z^2 \rangle$  and  $\langle a_x^2 \rangle$  as well as cross terms such as  $\langle a_z a_x \rangle$ . For simple crystal structures, normally the in-plane cross correlations vanish, i.e.,  $\langle a_y a_x \rangle = 0$ , but the broken symmetry in the spatial dimension normal to the surface allows for  $\langle a_z a_x \rangle \neq 0$ . However, it is a reasonable approximation to assume that these cross terms are small. In

order to simplify to a characteristic function for attenuation that depends on only a single parameter, one can adopt the assumption

$$\langle a_z^2 \rangle = \langle a_x^2 \rangle = \langle a_y^2 \rangle = a^2, \quad (17)$$

where  $a$  is the root-mean-square displacement  $a = \sqrt{\langle a_z^2 \rangle}$ . With these assumptions, the diffraction peaks are modified by a very simple attenuation function so that Eq. (13) becomes

$$I_{\mathbf{G}} = I_{\mathbf{G}}^0 e^{-\Delta\mathbf{k}^2 a^2}, \quad (18)$$

and the dependence of the attenuation function on  $\mathbf{G}$  is now contained in  $\Delta\mathbf{k}^2$ . The above is the single parameter expression used in this paper for analyzing the disorder attenuation of the diffraction data.

Some remarks and ramifications of the results obtained here are in order. The characteristic attenuation function of Eq. (13), or its simplified form of Eq. (18), is not the only form that can be obtained. Equation (13) was obtained under the assumption that the small static displacements of each unit cell, i.e.,  $\mathbf{a}_{\ell}$ , were random and governed by a Gaussian distribution function. The result is that the attenuation factor of Eq. (13) looks very similar to the Debye-Waller attenuation factor obtained for bulk neutron or X-ray scattering and also adapted to atom and molecule scattering from surfaces. The form of the Debye-Waller-like attenuation is also due to the fact that the dynamical roughening induced by phonon displacements at a particular unit cell of a periodic surface likewise obeys a Gaussian distribution function. Thus in the present case, the static roughness displacement  $\mathbf{a}_{\ell}$  takes the place of the phonon displacement in the Debye-Waller factor. However, an attenuation factor having Debye-Waller-like appearance is not the only possibility. Other assumptions on the distribution function of the static roughness lead to other forms of the characteristic function of attenuation.<sup>21</sup> However, since the distribution function applies only to the roughness parameter  $\mathbf{a}_{\ell}$ , then it is only the attenuation factor in the diffractive transition rate of Eq. (12) that would change, and the remaining factors of that equation remain the same.

An additional remark is to note that in the derivation of the diffractive transition rate of Eq. (12), it was assumed that each surface unit cell was capable of small displacements. This is not the only type of disorder that gives rise to similar types of attenuation as that discussed here. For example, suppose the surface is made up of rigid or frozen islands, each containing many unit cells, but each island has a small random roughness displacement. In other words, within each island all unit cells have the same displacement, but the islands themselves have random displacements with respect to each other. This model can be treated similarly to the simpler treatment given here, and the result is similar to the attenuated diffraction intensities given in Eq. (12).

### C. Potential energy surface

As discussed in Ref. 15, two candidate SRP density functionals were derived for  $\text{H}_2 + \text{Ru}(0001)$ . Since these were rather similar, here we will consider only one of them, i.e., the one that was called the PBE:RPBE(50:50)-vdW-DF functional. The exchange-correlation part of this functional can be

written as

$$E_{XC} = xE_X^{RPBE} + (1-x)E_X^{PBE} + E_C^{vdW-DF}, \quad (19)$$

where  $E_X^{RPBE}$  is the exchange part of the RPBE functional,<sup>12</sup>  $E_X^{PBE}$  is the exchange part of the PBE functional,<sup>27</sup> and the non-local correlation functional  $E_C^{vdW-DF}$  of Dion *et al.*<sup>28</sup> was used to approximately describe the attractive van der Waals interaction. The value  $x = 0.5$  was found<sup>15</sup> to yield an accurate description of molecular beam experiments of sticking of H<sub>2</sub> and D<sub>2</sub> on Ru(0001) at normal incidence.<sup>16</sup> Here we will call this functional the cSRP50-vdW functional, where “50” stands for the RPBE mixing ratio in percent, “cSRP” stands for candidate SRP functional, and “vdW” refers to the use of the correlation functional of Dion *et al.*<sup>28</sup>

To build the potential energy surface (PES) used in the dynamics calculations, DFT calculations were performed with Vienna Ab-Initio Simulation program (VASP).<sup>29–33</sup> The DFT calculations employed a 5-layer Ru slab and a  $2 \times 2$  surface unit cell with a vacuum of 13 Å between images of the slab. An  $8 \times 8$   $\Gamma$ -centered Monkhorst-Pack grid was used in the k-point integration and a plane-wave cutoff of 350 eV. More computational details can be found in the original paper.<sup>15</sup>

To obtain the PES, the DFT data were interpolated with the corrugation reducing procedure (CRP)<sup>34</sup> as described in full detail in Ref. 15. Figure 4 and Table I give some details of the PES. As can be seen, the barrier to dissociation shows corrugation, i.e., the barrier height is different for different corrugation sites and dissociation geometries. The minimum barrier height  $E_b$  for dissociation is only 4 meV and occurs for dissociation over the top site. Note that for some sites there is only one barrier along the reaction path (e.g., the bridge and hcp sites), while on other sites two barriers are encountered moving along the reaction path (e.g., the top and t2h sites).

TABLE I. Transition state geometries ( $r_b$ ,  $Z_b$ ) and energies ( $E_b$ ) computed<sup>15</sup> with the cSRP50-vdW functional, relative to the gas phase minimum, for the four geometries depicted in Fig. 4. Where a second barrier (2) is present, results for this barrier are also given.

Parameter	Top 1	Top 2	t2h 1	t2h 2	bri	hcp
$\phi$ (deg)	0	0	120	120	90	30
$r_b$ (Å)	0.751	1.249	0.771	1.072	0.799	0.861
$Z_b$ (Å)	2.605	1.559	2.122	1.474	1.830	1.646
$E_b$ (eV)	0.004	-0.044	0.125	0.096	0.295	0.459

In Fig. 5, the potential for H<sub>2</sub> interacting with Ru(0001) is shown as a function of  $Z$  for  $r$  equal to its gas phase equilibrium value, with averaging over the other four H<sub>2</sub> degrees of freedom. The van der Waals interaction potential that is averaged over orientation angles and impact points on the surface has a minimum well depth of 52.7 meV, in rather good agreement with the value derived experimentally from the DW attenuation factor ( $60 \pm 5$  meV),<sup>6</sup> the minimum being located at  $Z = 3.7$  Å.

#### D. Dynamics calculations

Diffraction probabilities were first computed<sup>15</sup> with the time-dependent wave packet (TDWP) method<sup>24</sup> in an implementation for scattering of diatomic molecules from a surface with hexagonal symmetry.<sup>25</sup> As in the reporting of the earlier experimental<sup>5,6</sup> and theoretical<sup>15</sup> results, the diffraction states were defined as appropriate for an fcc metal, even though Ru is an hcp metal (see Fig. 3). Results were measured and computed for two high symmetry incidence directions, i.e., the  $[10\bar{1}]$  and the  $[11\bar{2}]$  directions, again using the conventions appropriate for fcc metals (see also Fig. 3). In the TDWP calculations, the application of scattering boundary conditions yields S-matrix

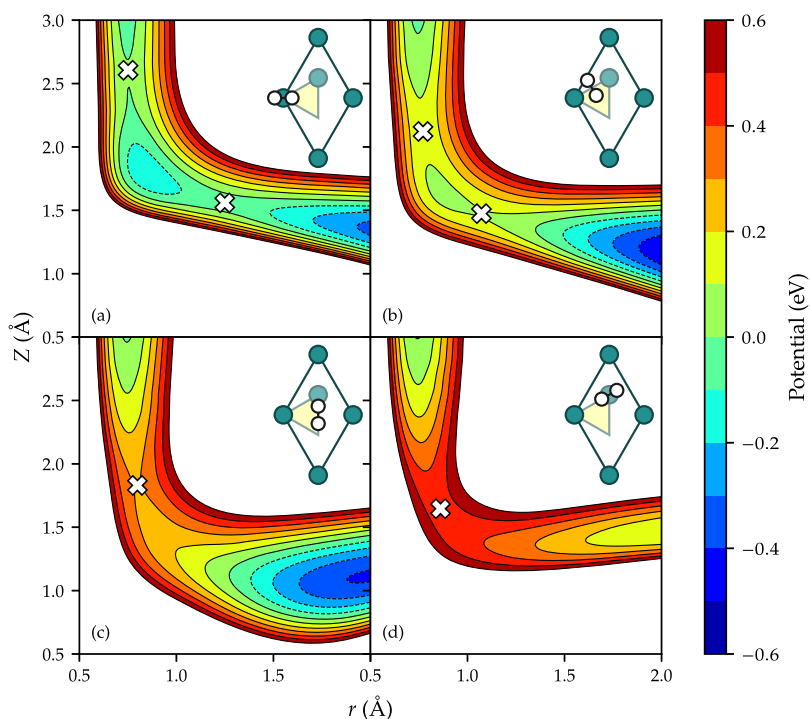


FIG. 4. Contour plots of the H<sub>2</sub> on Ru(0001) PES for four high symmetry configurations with H<sub>2</sub> parallel to the surface, for the cSRP50-vdW functional. Transition states are indicated by crosses. The spacing between contour lines is 0.1 eV.

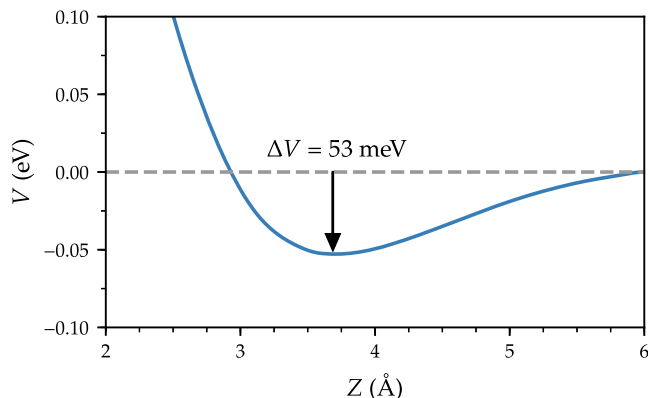


FIG. 5. The cSRP50-vdW potential for  $\text{H}_2 + \text{Ru}(0001)$  is shown as a function of  $Z$  in the region of the van der Waals well, for  $r = r_e$ , after averaging over the four remaining molecular degrees of freedom.

elements, and the absolute squares of the S-matrix elements yield the probabilities for rotationally elastic diffractive scattering  $P(v = 0, j, m_j \rightarrow v' = 0, j', m_{j'}, n, m)$ , where  $v(v')$ ,  $j(j')$ , and  $m_j(m_{j'})$  are the initial (final) values over the vibrational, rotational, and magnetic rotational quantum numbers, respectively. These probabilities are summed over  $m_{j'}$  and averaged over the  $m_j$  states. To simulate the diffractive scattering of  $n\text{-H}_2$  from an ideal 0 K surface, calculations were carried out for  $j = 0$   $\text{H}_2$  modeling the  $p\text{-H}_2$  contribution (weight 0.25) and  $j = 1$   $\text{H}_2$  modeling the  $o\text{-H}_2$  contribution (weight 0.75), obtaining rotationally elastic diffraction probabilities  $P_{nm}$ . All measurements and calculations were carried out for an initial parallel translational energy of 35 meV (for one and the same initial parallel energy, TDWP results can be obtained for a large range of  $E_i$  from a single wave packet calculation<sup>25,35</sup>). Using Eq. (18), diffraction probabilities for scattering from a surface affected by static surface disorder can then be computed from

$$P'_{nm} = e^{-Ak^2a^2} P_{nm}. \quad (20)$$

All technical details of the TDWP calculations have been presented in Ref. 15.

### III. RESULTS AND DISCUSSION

#### A. Comparison theory–experiment: The effect of static surface disorder

The computed diffraction probabilities with and without<sup>15</sup> correction for static disorder are compared with experimental diffraction probabilities obtained by applying the usual thermal Debye-Waller extrapolation corrections<sup>15</sup> in Fig. 1. The static disorder attenuation parameter  $a$  was obtained by demanding that the corrected specular scattering probabilities should be in good agreement with experiment. This gave a value of 0.1 bohr for  $a$ , and with this value the corrected computed specular scattering probabilities are in quite good agreement with the experimental values. The uncorrected computed values of the specular scattering probabilities overestimate the experimental values by factors of 2 and 3, with the discrepancy increasing with the incident normal energy.<sup>15</sup>

As can be seen from Fig. 1, the static disorder correction also yields a much improved description of the other diffraction channels. The only channels for which the agreement with experiment remains rather poor after correction for static disorder are the forward and forward-sideways scattering channels, i.e., the (11) channel for the  $[11\bar{2}]$  incidence direction and the sums of the probabilities for the (10) and (01) channels for the  $[11\bar{2}]$  direction and for the (11) and (10) channels for the  $[10\bar{1}]$  incidence direction. For these channels, the agreement between the corrected computed probabilities and the experimental diffraction probabilities, although improved, is still poor for the entire range of incidence energies ( $E_i$ ). For the remaining diffraction channels, the agreement with experiment is much improved, especially for normal incidence energies  $\geq 60$  meV.

#### B. Discussion

In Sec. III A, we have established that an improved description of the diffraction experiments can be obtained if the assumption is made that at the surface temperature and other conditions at which the measurements were taken,<sup>5,6</sup> the surface is affected by a specific type of static surface disorder. However, we have not yet discussed in great detail what kind of form this static surface disorder could take or whether it is plausible that the actual experiments could have suffered from such a “problem.” This will be done in the present section, in which we will also consider alternative causes for the remaining discrepancies, which either taken by themselves or taken in conjunction with static surface disorder could perhaps explain the discrepancies remaining with the measured (and Debye-Waller extrapolated) diffraction probabilities.

One way of thinking about the static surface disorder parameter  $a$ , which we have fitted to the specular scattering probabilities, is that it describes a small static root-mean-square displacement “ $a$ ” of each and every primitive unit cell on the Ru(0001) surface and that this displacement is temperature-independent over the range of  $500 \leq T_s \leq 1000$  K. However, it is not clear how such a static type of surface disorder could arise. Nevertheless one can show that the exact same attenuation expression as described in Sec. II B can be obtained under physically more plausible conditions, if the following 3 assumptions are made: (i) the surface can be divided up into large domains, each containing many primitive surface unit cells, (ii) each domain has a root-mean-square displacement “ $a$ ” with respect to the other domains, and this displacement is Gaussian (randomly) distributed, and (iii) each domain within itself remains on the same plane. In principle, such a situation could arise if a surface has steps and terraces with differing heights, and the ensuing static surface disorder would then cause the attenuation described in Fig. 1.

The question then arises whether a static disorder of the Ru(0001) surface, characterized by  $a = 0.1$  bohr, could be present in the diffraction experiments. Of these, the following can be said. The Ru(0001) crystal has a miscut of  $0.1^\circ$  so that in principle the width of the terraces should be in the range 50-70 nm.<sup>36</sup> It is not clear why the resulting low



step density should then lead to the quoted static disorder parameter of 0.1 bohr. On the other hand, it is known that the adsorption of H<sub>2</sub> to Ru(0001) can lead to greater surface roughness, as expressed by the Debye-Waller factor and  $\beta$ -roughness parameter measured with X-ray diffraction, where the latter parameter is indicative of the presence of steps.<sup>37</sup> In other words, hydrogen adsorption (which will occur to some extent in the diffraction experiments) may lead to increases in the number of steps. However, the experiments measuring a higher  $\beta$ -roughness parameter were done for a surface coverage of 0.33 ML, and the  $\beta$ -roughness parameter resumed its original clean surface value upon desorption of H<sub>2</sub> at 490 K.<sup>37</sup> The H<sub>2</sub> diffraction experiments were done for  $T_s = 500$  K, and assuming a sticking coefficient of 0.5 for  $E_i$  used in these experiments, with the incident H<sub>2</sub> flux used the surface coverage of Ru(0001) should be approximately 0.01 ML.<sup>5</sup> It is not clear whether such a low coverage of Ru(0001) by hydrogen could lead to the static disorder parameter suggested by the present work; we do not consider it likely. The nature and size of steps on the surface can be investigated using the so-called “drift-spectra” experiments similar to the ones that have been done in He atom scattering,<sup>38</sup> and originally carried out using Low Energy Electron Diffraction (LEED).<sup>39</sup> In such experiments, a controlled variation of the incident normal energy is used to induce a continuous change in the incident wave vector, and subsequent measurements of both intensity and widths of the diffraction peaks provide information on the distribution of steps.

Having discussed whether the amount of static surface disorder characterized by  $a = 0.1$  bohr is feasible (a question that remains open), it remains to discuss other sources of error. These errors might either account for the discrepancies that remain with the experiments after static surface disorder is taken into consideration as done here or account for the discrepancies with experiment while not or only in part considering static surface disorder. One way in which discrepancies between theory and experiment can arise where the theory is off from experiment by larger factors at high normal incidence energies (as observed if static surface disorder is not taken into account) is through errors made in the Debye-Waller extrapolation. The experimentally determined Debye-Waller factors (DW factors) were analyzed through the following expression, similar to Eq. (18), used to describe the fitted diffraction intensities,

$$I_G = I_G^0 e^{-2W(T_s)}, \quad (21)$$

where again  $I_G^0$  is the diffraction intensity expected for a rigid frozen surface and  $2W(T_s)$  is the Debye-Waller exponent. In molecular beams scattering the DW exponent is often approximated by the following expression, borrowed from the theory of neutron scattering:

$$W(T_s) = 12m(E_i \cos^2 \theta_i + D)T_s / (Mk_B \Theta_D^2). \quad (22)$$

In Eq. (22), which is a form specific to the specular beam,  $m$  is the mass of the H<sub>2</sub> projectile,  $M$  is the effective mass of the surface,  $\Theta_D$  is the surface Debye temperature, and the parameter  $D$  is the depth of the attractive van der Waals well. Assuming an effective surface mass  $M$  equal to that of a single Ru atom, the van der Waals well depth was evaluated as  $60 \pm 5$  meV,<sup>6</sup> in reasonable agreement with the value of 53 meV

computed by us. The surface Debye temperature  $\Theta_D$  was fitted to  $473 \pm 2$  K,<sup>6</sup> in not so good agreement with the values of 321 K determined by Madey *et al.*<sup>40</sup> and of  $295 \pm 10$  K for the first layer of Ru(0001) by Ferrari *et al.*<sup>41</sup> However, the evaluation of the various parameters in Eq. (22) is unimportant because in the DW extrapolation the only information used is the temperature dependence of the DW factor. In other words, Eq. (21) becomes effectively

$$I_G = I_G^0 e^{-C_G T_s}, \quad (23)$$

where  $C_G$  is a different constant for each diffraction peak, which additionally depends on incident energy and angle. This temperature dependence, as opposed to the other parameters in Eq. (22), is exact within the harmonic approximation for the vibrations of a crystal lattice because it arises from the mean square phonon amplitude, which at sufficiently large temperatures is directly proportional to  $T_s$ . Thus, any uncertainties in the temperature extrapolation arise from the experimental errors in determining the constant  $C_G$  for each diffraction peak. However, as is evident from the discussions of the DW extrapolations associated with Fig. 6 of Ref. 6, these uncertainties are far too small to explain the observed discrepancies.

The way in which the rotational distribution of H<sub>2</sub> in the molecular beam is approximated in the theory represents another source of error. In the experiments, the nozzle temperature is varied between room temperature and 600 K to achieve  $E_i$  ranging from 78 to 150 meV. Assuming that the rotational temperature of H<sub>2</sub> in the beam  $\approx 0.8$  times the nozzle temperature,<sup>20</sup> roughly 88% of the molecules should be in the  $j = 0$  (18%) and the  $j = 1$  (71%) states at the lowest  $E_i$  and 67% of the molecules should be in the  $j = 0$  (12%) and the  $j = 1$  (55%) states at the highest  $E_i$ . However, the theory approximated the rotational state distribution of the beam as consisting of 25%  $j = 0$  and 75%  $j = 1$  H<sub>2</sub>. If  $j = 2$  and  $j = 3$  H<sub>2</sub> were to show more rotationally inelastic scattering or reaction than  $j = 0$  and  $j = 1$  H<sub>2</sub>, this could lead to smaller computed probabilities for diffraction for all final states investigated and to better agreement between the computed rotationally elastic diffraction probabilities and the DW extrapolated experimental values in Fig. 1. However, even if  $j = 2$  and  $j = 3$  H<sub>2</sub> would show no rotationally elastic diffraction at all, the theory would still overestimate the DW extrapolated rotationally elastic diffraction probabilities, especially at high  $E_i$ . The reason for this is that the theory now overestimates these experimental probabilities by factors of 2 and 3, while the rotational states now contributing to the theoretical results ( $j = 0$  and  $j = 1$ ) make up about 67% of the molecules in the beams at the highest  $E_i$  and a larger percentage at lower  $E_i$ . Note that we expect the relative values of the rotationally elastic diffraction probabilities  $P(v = 0, j \rightarrow v' = 0, j' = j, n, m)$  to be, to good approximation, independent of  $j$ , as, from an electronic density point of view, H<sub>2</sub> is almost a spherical particle.<sup>42</sup> Nevertheless it would be of interest to see, in future calculations, how the computed rotationally averaged diffraction probabilities would change if the scattering of  $j = 2$  and  $j = 3$  H<sub>2</sub> would also be taken into account. Calculations with another functional that is good at describing reaction of H<sub>2</sub> on Ru(0001) suggest that relative to  $j = 0$  and  $j = 1$  H<sub>2</sub>, the reaction probability of  $j = 2$  and  $j = 3$

$H_2$  should be somewhat smaller. It is not clear how the total probability of rotationally inelastic scattering would change, but we do not expect major effects as in any case most of the rotationally inelastic scattering should be between  $j = 0$  and 2 and between  $j = 1$  and 3, in view of the large rotational constant of  $H_2$ .

Finally, it is possible that the PES we used, while good at describing reaction of  $H_2$  on Ru(0001),<sup>15</sup> is not good at describing the rotationally elastic diffractive scattering. While we cannot completely rule this out, it is unlikely that the PES should constitute a major source of error. First, for the PES to be able to accurately describe the reaction probability over the rather large range of normal incidence energies for which experiments and calculations were done (approximately 70–470 meV, this range also overlaps the range of normal incidence energies addressed in the present diffraction experiments, i.e., 43–115 meV), the PES has to describe reasonably well how the barrier height varies with the orientation of  $H_2$  and with its impact site on the surface. This would make it rather unlikely that the PES shows much too little rotational anisotropy (more anisotropy would lead to more rotationally inelastic scattering, and therefore too little computed rotationally elastic diffraction, which would enhance the agreement with the DW extrapolated measured diffraction probabilities). In this connection, it should also be noted that the SRP density functional for  $H_2 + Cu(111)$ , which was fitted to sticking experiments, also provided quite a good description of rotationally inelastic scattering of  $H_2$  from Cu(111).<sup>13</sup> For the same reason, we find it rather unlikely that the PES we used for  $H_2 + Ru(0001)$  should exhibit way too much or too little corrugation, which would alter the relative values of the rotationally elastic diffraction probabilities.

Perhaps a clue may be found in the good agreement previously achieved for specular and first order diffractive scattering of  $H_2$  from Pt(111).<sup>7</sup> More specifically, for this case, a semi-quantitative agreement was obtained between computed and DW extrapolated measured diffraction probabilities (much better than observed here), while the agreement between computed<sup>7</sup> and measured<sup>17</sup> reaction probabilities was likewise rather good (semi-quantitative). However, in this case the PES that was used was computed with a generalized gradient approximation (GGA) functional (the Becke-Perdew functional).<sup>43,44</sup> This functional does not yield an approximately correct description of the van der Waals interaction; in fact, no van der Waals well is present in the Becke-Perdew PES for  $H_2 + Pt(111)$ .<sup>45,46</sup> By contrast, in more recent calculations on  $H_2 + Pt(111)$  with an SRP functional yielding a van der Waals well, excellent agreement with sticking data<sup>17</sup> was achieved, but the description of diffraction experiments<sup>7</sup> was rather poor.<sup>18</sup> From a sticking point of view, the  $H_2 + Pt(111)$  and Ru(0001) systems are rather similar. This then raises the question of whether the present problem with the comparison between theory and experiment comes from using a static surface approximation in the dynamics and a PES exhibiting a van der Waals well to compare with experimental diffraction probabilities measured at 500 K and DW extrapolated to 0 K.

The potential existence of such a problem can be argued as follows. At 500 K, it may well be that the diffraction of  $H_2$  is

not affected much by indirect scattering on either Ru(0001) or Pt(111), where, in a classical picture, there would be scattering events involving multiple bounces of  $H_2$  with the surface. In this context, we note that the selective adsorption measured for hydrogen scattering from a Pt(111) surface at 500 K by Cowin *et al.* involved rotationally mediated selective adsorption of HD<sup>47,48</sup> and not corrugation mediated selective adsorption of  $H_2$ . However, in calculations within a static surface approximation that use a PES with a van der Waals well of  $\approx 50$  meV present, indirect scattering would be expected to occur. The question then arises whether it would be appropriate to use DW extrapolation of these static surface diffraction probabilities from, effectively, 0 K to the experimental surface temperature (which should be the same as DW extrapolating the measured diffraction probabilities from 500 K to 0 K as done here). In principle, the answer is no because the DW attenuation model is based on the molecule undergoing a single impulsive collision with the surface and is not applicable if “multiple collision effects” exist.<sup>49</sup> If in at least a fraction of the collisions there should be more than a single bounce, then in a classical picture there should be a larger probability of attenuation of the diffraction by a phonon-inelastic event than in a single bounce. Modeling this possible effect could lead to better agreement with experiment for  $H_2 + Ru(0001)$ , as presently the computed static surface diffraction probabilities overestimate the DW extrapolated measured diffraction probabilities.

The above stated reservations regarding the appropriateness of the use of DW attenuation in the presence of a van der Waals well facilitating indirect scattering are based on classical arguments. However, the  $H_2 + Ru(0001)$  data being considered here within the Born-Oppenheimer and static surface approximations are fully in the quantum mechanical regime as evidenced by the presence of prominent diffraction features. Thus, rebounding excursions of the  $H_2$  molecules into the van der Waals well occur as selective adsorption resonances, either diffraction or rotation mediated. The temperature dependence of isolated selective adsorption resonances has been investigated in the case of He atom scattering from a metal surface [Cu(115)], and it was found that the thermal attenuation near resonance conditions can indeed differ substantially from standard DW behavior.<sup>50</sup> It is hard to extrapolate this finding to the present  $H_2 + Ru(0001)$  system, as the incidence energies considered here are higher, so is the van der Waals well depth. Estimating the contributions of the resonances, which occur as peak-and-valley features in Fig. 1, is not very useful in this context: these features may look very differently in a calculation where the effects of surface phonons and surface temperature are modeled directly, and not through DW attenuation.

The existence of the potential problem mentioned above can be explored with calculations aimed at directly calculating diffraction probabilities for  $H_2$  scattering from a thermal surface, i.e., by modeling the effect of surface phonon motion on the diffraction directly, for the experimental surface temperature, and with quantum dynamics. Presumably, this could be done with quantum dynamics calculations in which at least the motion of first layer (and possibly second layer) surface atoms perpendicular to the surface is modeled, in seven-dimensional

(7D) (or eight-dimensional) quantum dynamics calculations also accurately describing the motion in all six molecular degrees of freedom, as has been done in 7D  $\text{H}_2 + \text{Cu}(111)$  calculations.<sup>51</sup> Alternatively, one might try to model the attenuating effect of phonons in 6D quantum dynamics calculations using a static surface approximation through the presence of a suitably chosen optical potential.<sup>52</sup> In yet another approach, in calculations on diffractive scattering one would “remove” the van der Waals well from the PES in a clever way and perform static surface calculations comparing with DW extrapolated measured probabilities, which is to some extent analogous to using a GGA PES. In such an approach, as in calculations using a GGA PES (without a van der Waals well), it would probably be more appropriate to apply Debye-Waller attenuation to the computed diffraction probabilities and to compare these to raw experimental data. In this context, more research is needed to arrive at a reliable quantum dynamical method for describing diffractive scattering from a thermal surface in a way that would either completely avoid the need for DW extrapolation for comparison with experiments, or make a comparison of computed DW attenuated probabilities with experiments feasible and useful for validating a PES. It is possible that with such a method one could arrive at an accurate comparison with the diffraction experiments on  $\text{H}_2 + \text{Ru}(0001)$ <sup>5,6</sup> without a need for invoking static surface disorder. Correcting for the other sources of error discussed above might lead to improved comparison with experiment in a context where static surface disorder of the  $\text{Ru}(0001)$  surface would also be taken into account.

#### IV. CONCLUSIONS AND OUTLOOK

We have considered whether a specific type of static surface disorder, which results in a random static displacement of the surface atoms by some specific value, can explain the discrepancy between diffraction probabilities computed within a static surface approximation and measured diffraction probabilities that were extrapolated to 0 K, for  $\text{H}_2 + \text{Ru}(0001)$ . The quantum dynamical calculations employed a PES computed with DFT, using a density functional that contains a 50:50 mixture of PBE and RPBE exchange and vdW-DF non-local correlation in the exchange correlation functional. The PES computed in this way contains a van der Waals well with a depth of approximately 53 meV. The experimental measurements were carried out for a surface temperature of 500 K and a parallel incidence energy of 35 meV for two high symmetry incidence directions, with the total incidence energy varying between 78 and 150 meV.

Without a correction for static surface disorder, computed specular and first order diffractive probabilities differed from the DW extrapolated measured probabilities by factors of 2 and 3. Taking static surface disorder into account using the static disorder parameter that was fitted to the specular scattering probabilities for the two incidence directions ( $a = 0.1$  bohr), much better agreement with the DW extrapolated measured probabilities was obtained. This agreement can be classified as semi-quantitative for all the investigated diffraction channels except for the forward and forward-sideways scattered channels.

Of course, an interesting question is whether the amount of static surface disorder implied by our calculations using  $a = 0.1$  bohr could have been present in the experiments. This is not impossible: it is known that the presence of hydrogen on  $\text{Ru}(0001)$  can lead to increased surface roughness, as characterized by a parameter indicating the amount of steps present on the surface. Hopefully experiments can be done in future to determine whether at the hydrogen coverage likely to be present under the experimental conditions of beam flux and surface temperature (about 0.01 monolayer) the surface is rough enough to affect the diffractive scattering to the extent suggested by our calculations assuming  $a = 0.1$  bohr.

We have also considered other possible sources of error in the previous comparison between theory and experiment. Errors arising from modeling  $n\text{-H}_2$  as a mixture of 25%  $j = 0$   $\text{H}_2$  and 75%  $j = 1$   $\text{H}_2$  and errors in the PES can affect the present comparison between the theory for the static surface and the DW extrapolated experimental measurements. However, we suggest that taken by themselves, these errors cannot account for the observed discrepancies, which amount to factors of 2 and 3. On the other hand, improving the theoretical description of the rotational state distribution in the beam and the accuracy of the PES together with a description of the effect of static surface disorder may well lead to further improved agreement between experiment and theory.

Perhaps a more important issue raised by the present and earlier studies concerns the principle of whether DW extrapolation can be used to facilitate the comparison between results of dynamics calculations using the static surface approximation and measurements on diffraction of  $\text{H}_2$  from a thermal metal surface at a temperature of  $\approx 500$  K, as we did here. There is a good reason for answering this question with “no” if the PES used in the dynamics calculations contains a van der Waals well so that indirect scattering can occur that cannot be described with a DW attenuation model. We suggest that models be developed that use a quantum dynamical method to compute diffraction probabilities directly for a thermal surface, by adding surface degrees of freedom or by modeling their attenuating effect through a suitably chosen optical potential. Alternatively, in calculations on diffractive scattering using a static surface model, it might be possible to remove the van der Waals well from the PES in a clever way, which would still allow measured diffraction probabilities to be used for validating semi-empirical density functionals derived from fits to sticking experiments.

#### ACKNOWLEDGMENTS

This work was supported financially by the division of Chemische Wetenschappen of the Nederlandse organisatie of Wetenschappelijk Onderzoek (NWO-CW) and by the European Research Council through an ERC-2013 advanced Grant (No. 338580) and with computer time granted by the Physical Sciences division of NWO (NWO-EW). G.J.K. thanks the Donostia International Physics Center (DIPC) for their generous financial support. We are grateful to Daniel Farías for useful discussions and to Davide Migliorini for providing us with Fig. 3.

- <sup>1</sup>D. Farías, H. F. Busnengo, and F. Martín, *J. Phys.: Condens. Matter* **19**, 305003 (2007).
- <sup>2</sup>M. Bertino and D. Farías, *J. Phys.: Condens. Matter* **14**, 6037 (2002).
- <sup>3</sup>D. Farías and R. Miranda, *Prog. Surf. Sci.* **86**, 222 (2011).
- <sup>4</sup>G. J. Kroes and C. Díaz, *Chem. Soc. Rev.* **45**, 3658 (2016).
- <sup>5</sup>P. Nieto, D. Barredo, D. Farías, and R. Miranda, *J. Phys. Chem. A* **115**, 7283 (2011).
- <sup>6</sup>P. Nieto, D. Farías, R. Miranda, M. Luppi, E. J. Baerends, M. F. Somers, M. J. T. C. van der Niet, R. A. Olsen, and G. J. Kroes, *Phys. Chem. Chem. Phys.* **13**, 8583 (2011).
- <sup>7</sup>P. Nieto, E. Pijper, D. Barredo, G. Laurent, R. A. Olsen, E. J. Baerends, G. J. Kroes, and D. Farías, *Science* **312**, 86 (2006).
- <sup>8</sup>D. Farías, C. Díaz, P. Rivière, H. F. Busnengo, P. Nieto, M. F. Somers, G. J. Kroes, A. Salin, and F. Martín, *Phys. Rev. Lett.* **93**, 246104 (2004).
- <sup>9</sup>C. Díaz, F. Martín, G. J. Kroes, M. Minniti, D. Farías, and R. Miranda, *J. Phys. Chem. C* **116**, 13671 (2012).
- <sup>10</sup>C. Díaz, R. A. Olsen, H. F. Busnengo, and G. J. Kroes, *J. Phys. Chem. C* **114**, 11192 (2010).
- <sup>11</sup>J. P. Perdew, J. A. Chevary, S. H. Vosko, K. A. Jackson, M. R. Pederson, D. J. Singh, and C. Fiolhais, *Phys. Rev. B* **46**, 6671 (1992).
- <sup>12</sup>B. Hammer, L. B. Hansen, and J. K. Nørskov, *Phys. Rev. B* **59**, 7413 (1999).
- <sup>13</sup>C. Díaz, E. Pijper, R. A. Olsen, H. F. Busnengo, D. J. Auerbach, and G. J. Kroes, *Science* **326**, 832 (2009).
- <sup>14</sup>G. J. Kroes, *J. Phys. Chem. Lett.* **6**, 4106 (2015).
- <sup>15</sup>M. Wijzenbroek and G. J. Kroes, *J. Chem. Phys.* **140**, 084702 (2014).
- <sup>16</sup>I. M. N. Groot, H. Ueta, M. J. T. C. van der Niet, A. W. Kleyn, and L. B. F. Juurlink, *J. Chem. Phys.* **127**, 244701 (2007).
- <sup>17</sup>A. C. Luntz, J. K. Brown, and M. D. Williams, *J. Chem. Phys.* **93**, 5240 (1990).
- <sup>18</sup>E. Nour Ghassemi, M. Wijzenbroek, M. F. Somers, and G. J. Kroes, *Chem. Phys. Lett.* **683**, 329 (2017).
- <sup>19</sup>H. A. Michelsen, C. T. Rettner, D. J. Auerbach, and R. N. Zare, *J. Chem. Phys.* **98**, 8294 (1993).
- <sup>20</sup>C. T. Rettner, H. A. Michelsen, and D. J. Auerbach, *J. Chem. Phys.* **102**, 4625 (1995).
- <sup>21</sup>P. Beckmann and A. Spizzichino, *The Scattering of Electromagnetic Waves From Rough Surfaces* (Pergamon Press, London, 1963).
- <sup>22</sup>M. Wijzenbroek, D. M. Klein, B. Smits, M. F. Somers, and G. J. Kroes, *J. Phys. Chem. A* **119**, 12146 (2015).
- <sup>23</sup>D. Farías and K. H. Rieder, *Rep. Prog. Phys.* **61**, 1575 (1998).
- <sup>24</sup>R. Kosloff, *J. Phys. Chem.* **92**, 2087 (1988).
- <sup>25</sup>E. Pijper, G. J. Kroes, R. A. Olsen, and E. J. Baerends, *J. Chem. Phys.* **117**, 5885 (2002).
- <sup>26</sup>H. Ibach and D. L. Mills, *Electron Energy Loss Spectroscopy and Surface Vibrations* (Academic Press, New York, 1982).
- <sup>27</sup>J. P. Perdew, K. Burke, and M. Ernzerhof, *Phys. Rev. Lett.* **77**, 3865 (1996).
- <sup>28</sup>M. Dion, H. Rydberg, E. Schröder, D. C. Langreth, and B. I. Lundqvist, *Phys. Rev. Lett.* **92**, 246401 (2004).
- <sup>29</sup>G. Kresse and J. Hafner, *Phys. Rev. B* **47**, 558 (1993).
- <sup>30</sup>G. Kresse and J. Hafner, *Phys. Rev. B* **49**, 14251 (1994).
- <sup>31</sup>G. Kresse and J. Furthmüller, *Phys. Rev. B* **54**, 11169 (1996).
- <sup>32</sup>G. Kresse and J. Furthmüller, *Comput. Mater. Sci.* **6**, 15 (1996).
- <sup>33</sup>G. Kresse and D. Joubert, *Phys. Rev. B* **59**, 1758 (1999).
- <sup>34</sup>H. F. Busnengo, A. Salin, and W. Dong, *J. Chem. Phys.* **112**, 7641 (2000).
- <sup>35</sup>G. J. Kroes and M. F. Somers, *J. Theor. Comput. Chem.* **4**, 493 (2005).
- <sup>36</sup>D. Farías, private communication (2016).
- <sup>37</sup>A. P. Baddorf, V. Jahns, D. M. Zehner, H. Zajonz, and D. Gibbs, *Surf. Sci.* **498**, 74 (2002).
- <sup>38</sup>B. J. Hinch, A. Lock, H. H. Madden, J. P. Toennies, and G. Witte, *Phys. Rev. B* **42**, 1547 (1990).
- <sup>39</sup>T.-M. Lu and M. G. Lagally, *Surf. Sci.* **120**, 47 (1982).
- <sup>40</sup>T. E. Madey, H. A. Engelhardt, and D. Menzel, *Surf. Sci.* **48**, 304 (1975).
- <sup>41</sup>E. Ferrari, L. Galli, E. Miniussi, M. Morri, M. Panighel, M. Ricci, P. Lacovig, S. Lizzit, and A. Baraldi, *Phys. Rev. B* **82**, 195420 (2010).
- <sup>42</sup>F. London, *Z. Phys.* **46**, 455 (1928).
- <sup>43</sup>A. D. Becke, *Phys. Rev. A* **38**, 3098 (1988).
- <sup>44</sup>J. P. Perdew, *Phys. Rev. B* **33**, 8822 (1986).
- <sup>45</sup>R. A. Olsen, G. J. Kroes, and E. J. Baerends, *J. Chem. Phys.* **111**, 11155 (1999).
- <sup>46</sup>R. A. Olsen, H. F. Busnengo, A. Salin, M. F. Somers, G. J. Kroes, and E. J. Baerends, *J. Chem. Phys.* **116**, 3841 (2002).
- <sup>47</sup>J. P. Cowin, C. F. Yu, S. J. Sibener, and J. E. Hurst, *J. Chem. Phys.* **75**, 1033 (1981).
- <sup>48</sup>J. P. Cowin, C. F. Yu, and L. Wharton, *Surf. Sci.* **161**, 221 (1985).
- <sup>49</sup>R. B. Gerber, *Chem. Rev.* **87**, 29 (1987).
- <sup>50</sup>G. Armand, J. Lapujoulade, and J. R. Manson, *Phys. Rev. B* **39**, 10514 (1989).
- <sup>51</sup>M. Bonfanti, M. F. Somers, C. Díaz, H. F. Busnengo, and G. J. Kroes, *Z. Phys. Chem.* **227**, 1397 (2013).
- <sup>52</sup>H. Chow and E. D. Thompson, *Surf. Sci.* **82**, 1 (1979).